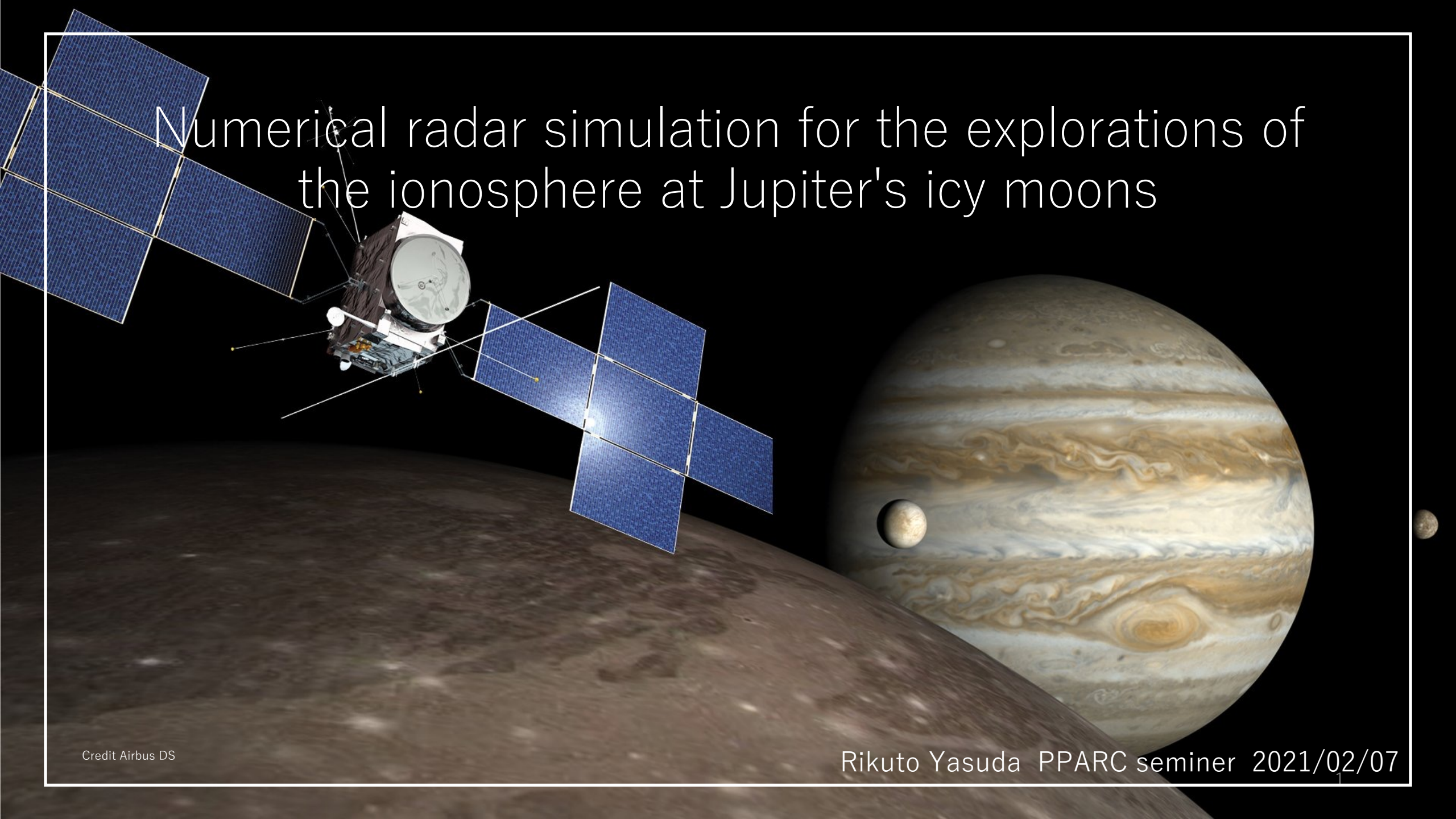


# Numerical radar simulation for the explorations of the ionosphere at Jupiter's icy moons



## 1. Introduction

1-1 [Jupiter's icy moon](#)

1-2 [Ionosphere of Jupiter's icy moon](#)

1-3 Previous observation of moon's ionosphere electron density

[1-3-1 Ganymede ionosphere](#)

[1-3-2 Europa ionosphere](#)

[1-3-3 Calisto ionosphere](#)

[1-3-4 Problems with the previous observation methods](#)

1-4 [Preceding studies of Jovian radio emission occultations](#)

1-5 [Purpose of this study](#)

## 2. Method

2-1 ExPRES

2-2 How to combine Raytracing method  
    with Radio Emission Simulations

2-3 Raytracing

2-4 Verify time-step validity of raytracing code

## 3. Radio occultation observation

3-1 [Ganymede ionosphere model](#)

3-2 [Ganymede ionosphere result](#)

3-3 [Discussion](#)

## 4. Conclusion

## 5. Future works

Reference

Appendix

# 1-1. Jupiter's icy moon

~ Jupiter's icy moon ~

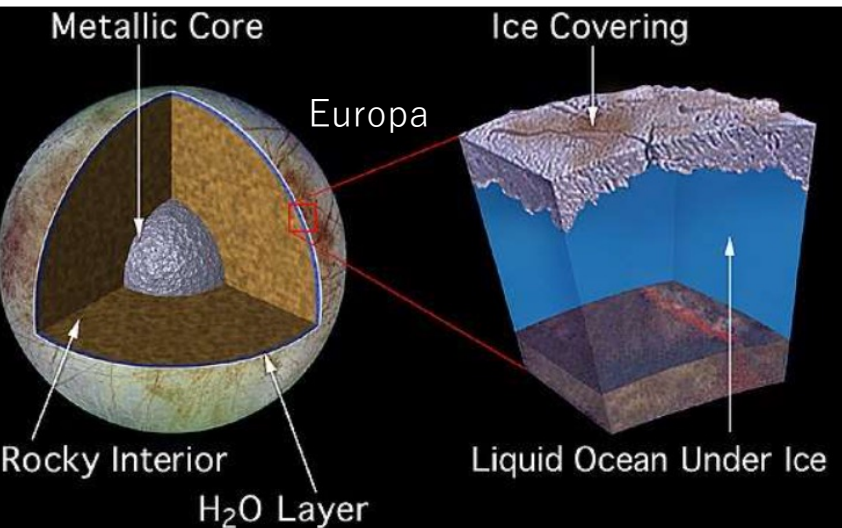
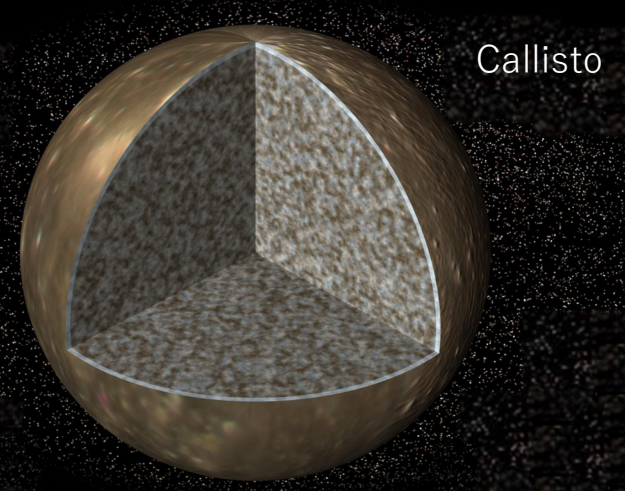
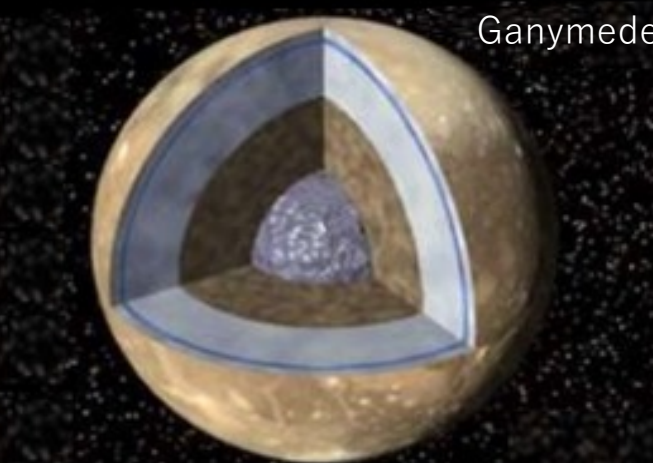


Fig.1 Model interiors of Ganymede Callisto and Europa [ Schubert et al, 2004]

## Jupiter's icy moon (ex. Europa, Ganymede, Callisto)

- possess internal liquid-water oceans [[Khurana et al., 1998](#); [Kivelson et al., 2002](#) etc..]
- Multiple icy bodies have subsurface ocean while only Earth has surface ocean.

Structures of the interior, ionosphere and plume of the icy moons are essential information for understanding universality of habitable environment.

It is impossible to observe directly ionosphere and plumes at low altitude as well as interiors.

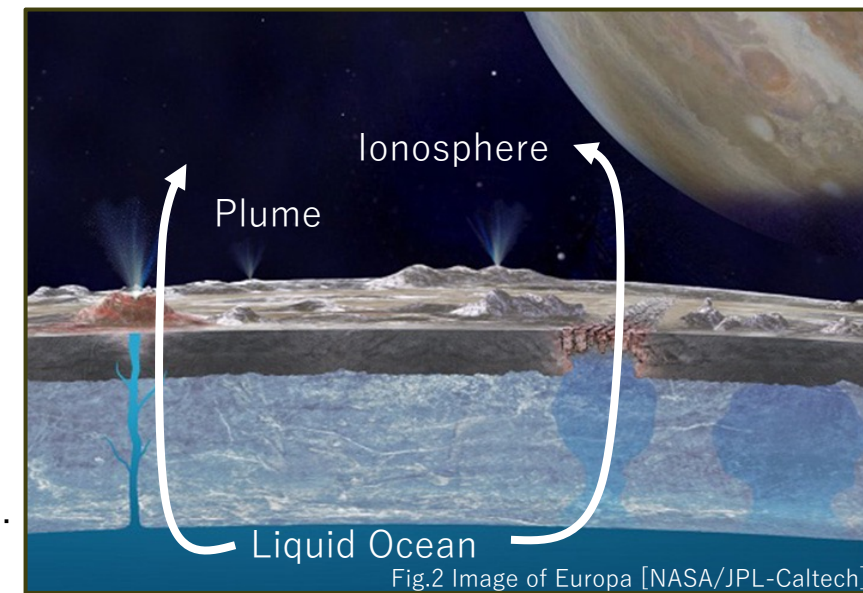


Fig.2 Image of Europa [NASA/JPL-Caltech]

# 1-1. Jupiter's icy moon

4

## JUICE (JUpiter ICy moons Explorer)

### Radio and Plasma Wave Investigation (RPWI) [Frequency: 80kHz~45MHz]

- ... A radio plasma wave instrument to characterize radio emission and plasma environment
- Apply to radio occultation observation or passive radar. (Fig.4, 5)



Fig.3 JUICE [Airbus DS]

#### ① Radio occultation observation of the ionosphere

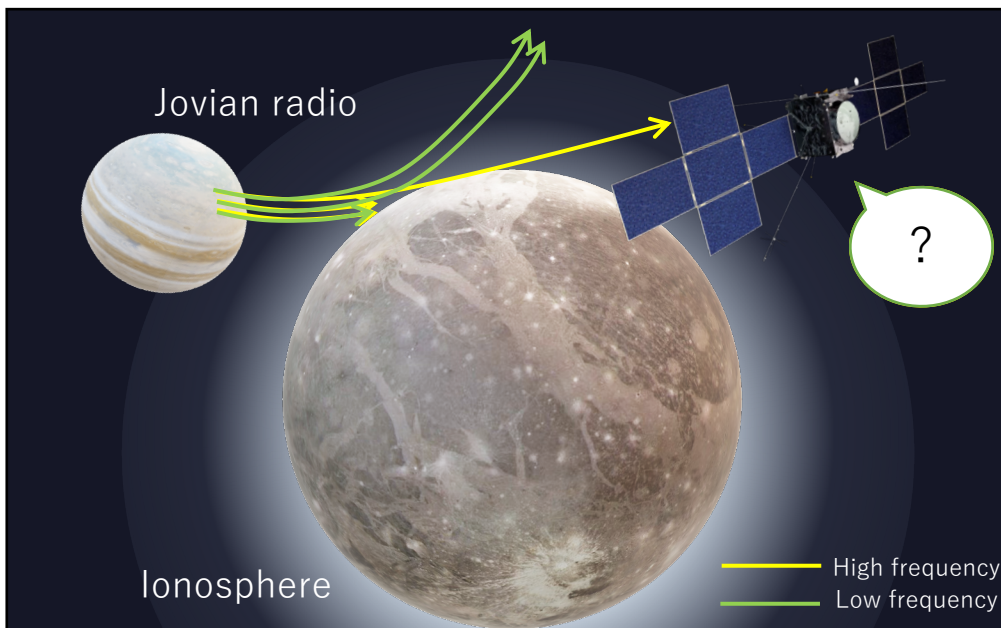


Fig.4 Radio observation using Jovian radio refraction  
(adapted from Airbus DS and NASA/JPL)

#### ② Passive radar

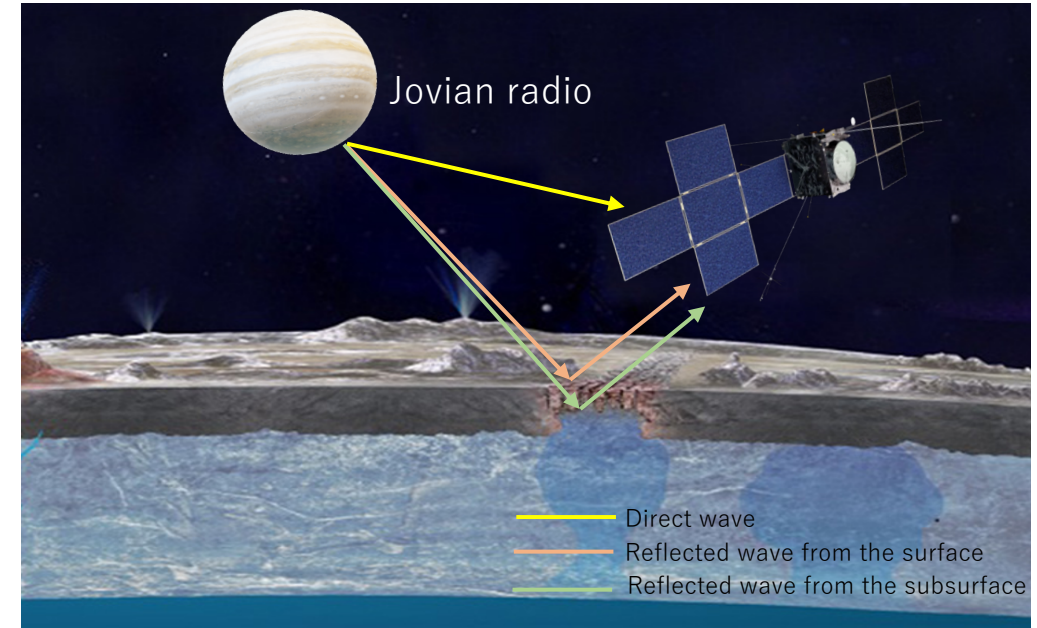
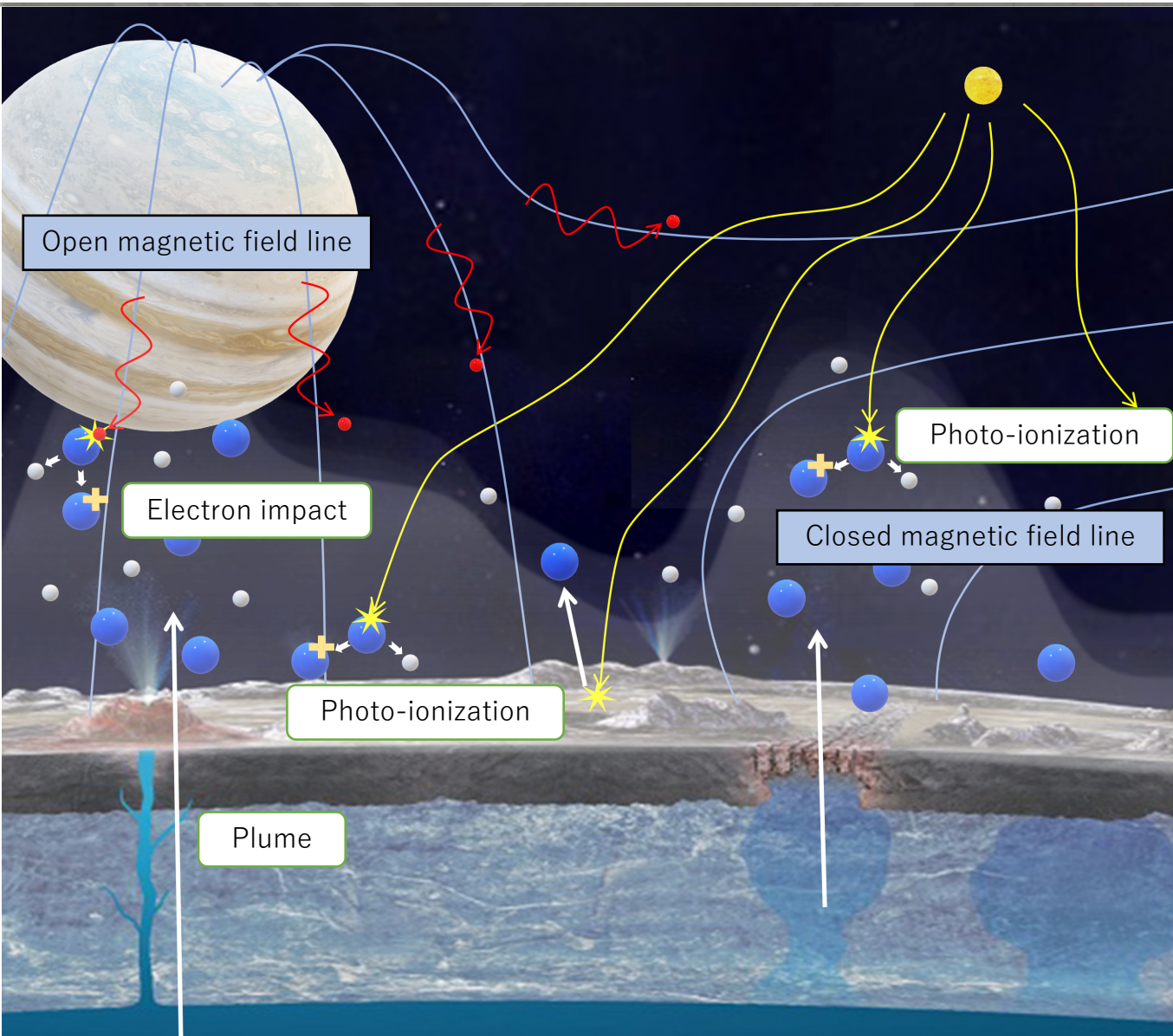


Fig.5 Radio observation using Jovian radio reflection  
(adapted from NASA/JPL, Airbus DS and gcoe-earths.org)

# 1-2. Ionosphere of Jupiter's icy moon



## Ionization source ([Carnielli et al. \(2019\)](#))

### ① Photo-ionization

exosphere is constantly photo-ionized by solar EUV radiation

### ② Electron impact

the energetic electrons (> tens of eV) are able to ionize the neutral exosphere.

## Ionosphere structure of icy moons

- Distribution of neutral atmosphere (and plume) created from oceanic water materials
- Solar photo-ionization rate and electron impact ionization rate ( Energy sources into icy moon )
- Open or closed magnetic field line (Ganymede)

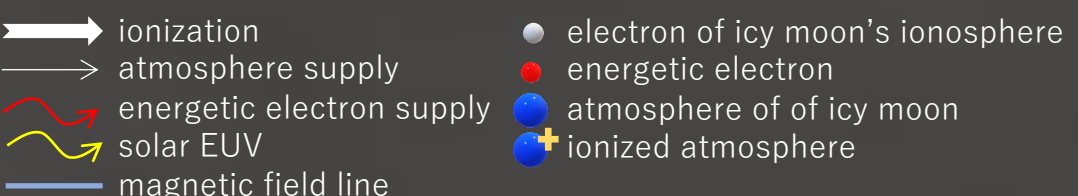


Fig. Ionization process of icy moon  
(adapted from NASA/JPL, Airbus DS and gcoe-earths.org)

# 1-3. Previous observation of moon's ionosphere electron density

6

## 1-3-1. Ganymede ionosphere

In-situ observation of Galileo flyby [Galileo plasma-wave instrument] (Fig.)

Upper hybrid resonance frequency  $f_{UH} = \sqrt{f_p^2 + f_c^2}$

When  $f_{UH} \gg f_c$ ,  $f_{UH} = f_p = 8980\sqrt{N}$  (Hz)

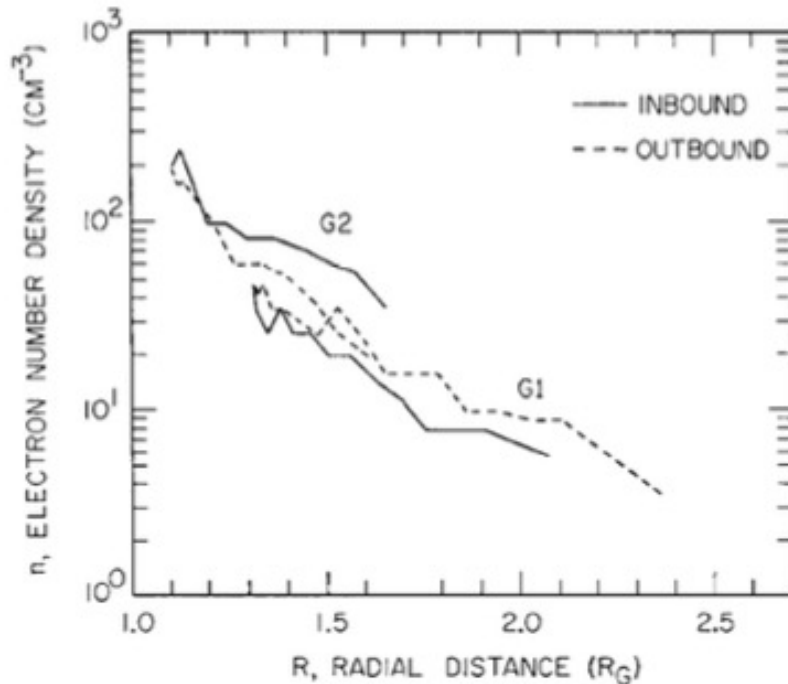


Fig. Electron density profiles on Ganymede 2 obtained by means of the PWS instrument on Galileo (Eviatar et al. 2001a)

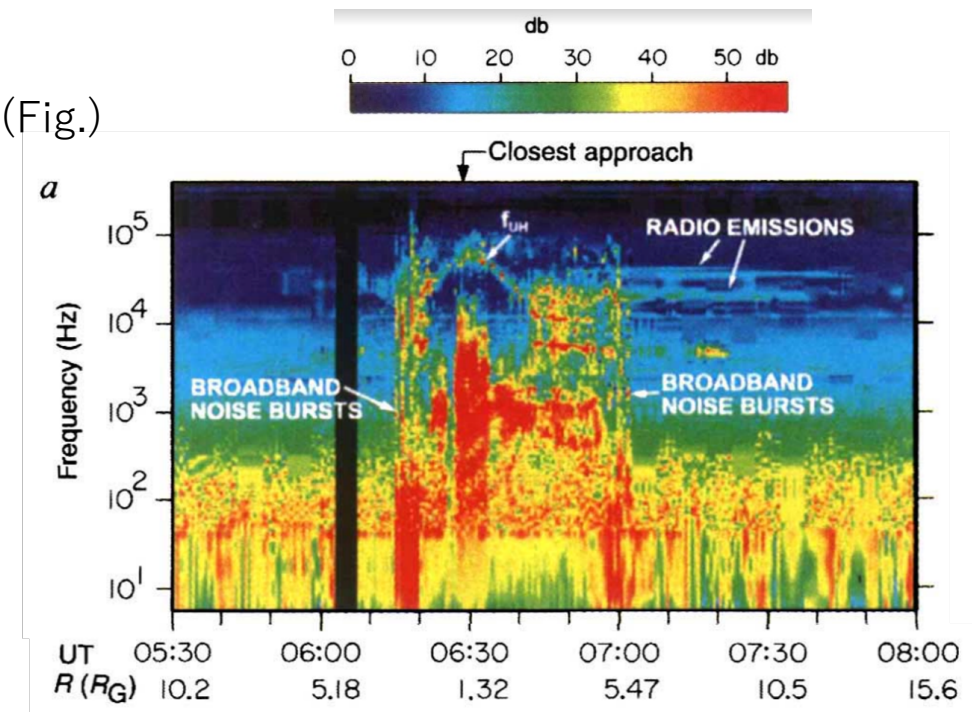


Fig. Frequency-time spectrograms of the electric field intensities detected by Galileo plasma wave instrument during the 27 June 1996 Ganymede fly-by (Eviatar et al. 2001a)

	Maximum densities	Scale height	
<a href="#">Gurnett et al. 1996</a>	~ 100 (/cc)	~1000 km	G1
<a href="#">Eviatar et al. 2001a</a>	~ 400 (/cc)	~600 km	G1&G2
<a href="#">Eviatar et al. 2001b</a>	~ 2500 (/cc)	~125km (near Ganymede) ~600 km (farther out)	G2

Fig. Proposed maximum electron densities and scale height of Ganymede ionosphere

# 1-3. Previous observation of moon's ionosphere electron density

7

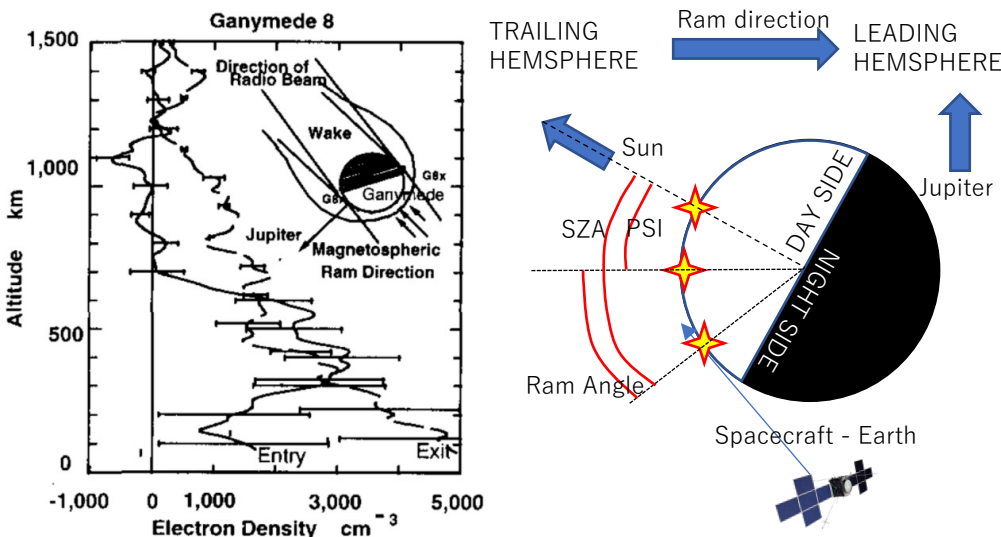
## 1-3-1. Ganymede ionosphere

Radio occultation [Galileo]

Maximum electron densities ...  $\sim 4000/\text{cc}$  ([Kliore 1998](#))

Observation	Lat (deg)	W. Long (deg)	SZA (deg)	Ram Angle (deg)
Ganymede 8 entry	41	201	82	69
Ganymede 8 exit	47	22	98	112

Fig. Geometry of Galileo occultations by Ganymede.



Only one strong detection ([McGrath et al. \(2004\)](#))

(strong detection 1/8 weak detection 2/8 non-detecton 5/8)

(The ionospheres of Ganymede and Callisto from Galileo radio occultations)

Fig. Electron density profiles for Ganymede  
([Kliore 1998](#))

Fig. Ram angle, SZA and PSI

[Carnielli et al. \(2019\)](#)

- ~ ([Eviatar et al., 2001](#)) presented electron density profiles from the Plasma Wave Science (PWS) instrument along the G1 and G2 flyby trajectories, consistent with the upper limit of [Kliore \(1998\)](#). ~
- ~ in the region of closed magnetic field lines we would expect mainly low energy electrons to be present from photo-ionization of the neutral atmosphere, and not energetic electrons from the Jovian plasma sheet which are not able to penetrate ~



Electron density distribution of ionosphere → What is the origin of Ganymede ionosphere?

# 1-3. Previous observation of moon's ionosphere electron density

## 1-3-2. Callisto ionosphere

Radio occultation [Galileo] ([Kliore et al. 2002](#))

Maximum electron densities

- ...  $15300 \pm 2300/\text{cc}$  (C22 entry • peak altitude  $\sim 27\text{km}$ )
- $17400 \pm 1500/\text{cc}$  (C23 entry • peak altitude  $\sim 48\text{km}$ )

Observation	Lat (deg)	SZA (deg)	Ram (deg)	Psi (deg)	detection
C9 entry	2.2	81.5	105.7	172.9	none
C9 exit	2.8	98.5	74.4	//	none
C20 entry	8.6	85.0	82.8	<b>2.4</b>	<b>weak+</b>
C20 exit	0.8	101.3	99.2	//	<b>weak+</b>
C22 entry	3.6	78.7	80.9	<b>2.1</b>	<b>strong++</b>
C22 exit	7.5	95.0	97.8	//	<b>weak+</b>
C23 entry	6.6	82.5	81.7	<b>1.0</b>	<b>strong++</b>
C23 exit	3.6	97.6	98.9	//	<b>weak+</b>

Fig. Geometry of Galileo occupations by Callisto.

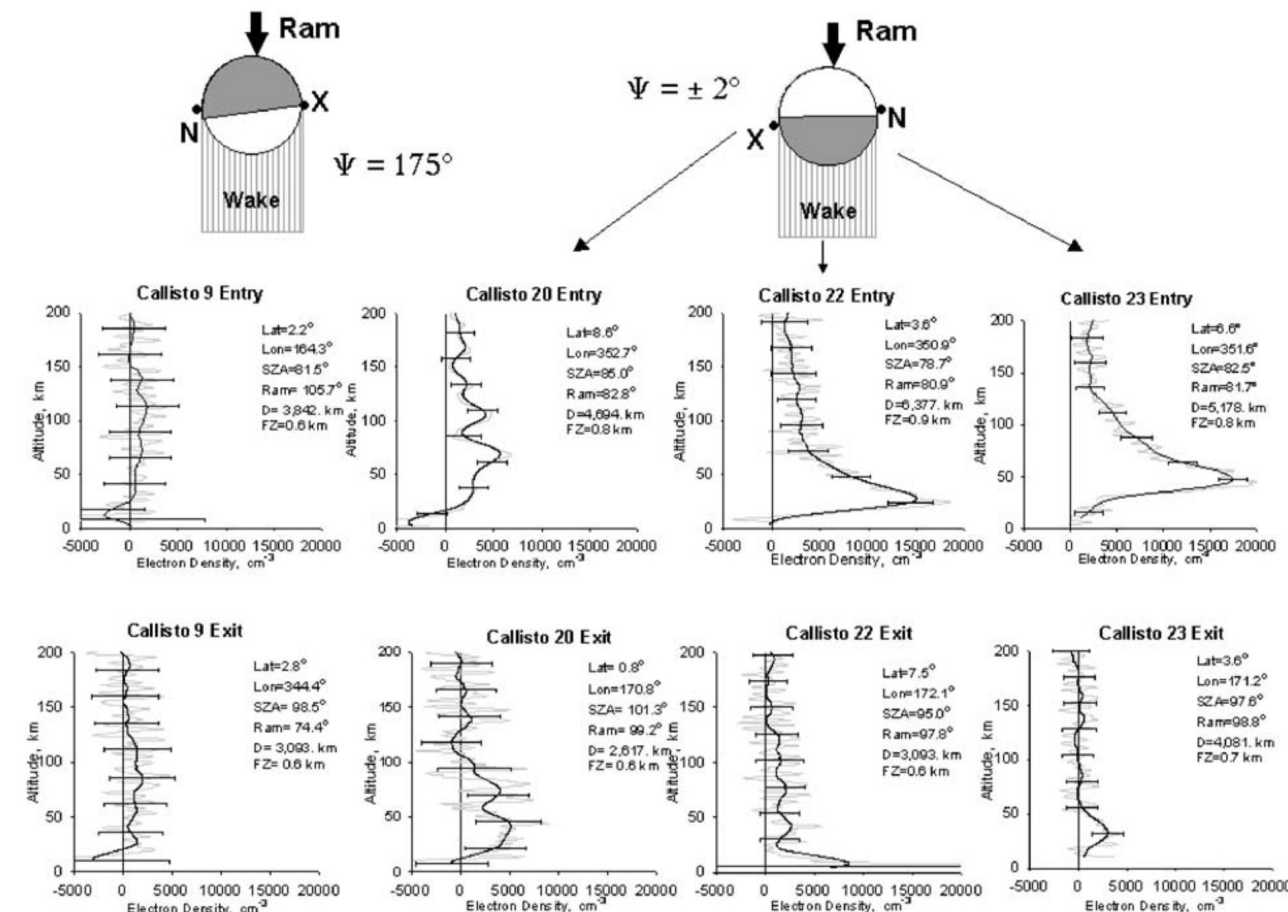


Fig. Electron density profiles for Callisto (Kliore et al. 2002)

It was found that the presence of a detectable ionosphere, at least in the equatorial terminator regions, coincided **with solar illumination of the trailing hemisphere** of Callisto.

# 1-3. Previous observation of moon's ionosphere electron density

## 1-3-2. Callisto ionosphere

In-situ observation of Galileo flyby [Galileo plasma-wave instrument]

Maximum electron densities ...  $\sim 400/\text{cc}$  C10 flyby • closest approach altitude 535km

([Gurnett et al](#) (2000))

$\sim 100/\text{cc}$  C3 flyby • closest approach altitude 1136km

([Gurnett et al](#) (1997))

Date	96/11/04	97/06/25	97/09/17	99/05/05	99/06/30	99/08/14	99/09/16	01/05/25
Flyby-No.	C3	C9	C10	C20	C21	C22	C23	C30
Magnetic	✓	✓	✓	x	✓	✓	✓	✓
Radio	x	✓	x	✓	x	✓	✓	x
Up/Down	Down	Up	Down	Down	Down	Down	Down	Down
Day/Night	Day	Night	Day	Night	Both	Night	Night	Both
C/A [km]	1136	418	535	1321	1048	2299	1052	132
$h_{CS} [R_J]$	3.24	-3.52	-2.45	2.93	-1.87	-4.31	1.08	3.50

Fig. Date of flyby (Date), flyby identification number (Flyby-No.), magnetometer measurement (Magnetic), radio occultation measurement (Radio), flyby passing the upstream or/and downstream side (Up/Down), flyby passing the day or/and night side (Day/Night), closest approach altitude (C/A), distance from the magnetospheric current sheet ( $h_{CS}$ ). ([Hartkorn](#) (2017))

[Gurnett et al](#) (2000)

- The closest approaches for C3 and C10, which had the highest plasma densities, were on the sunlight side of the moon
- the closest approach for C22, which had very low plasma densities, was on the dark side of the moon

This local time dependence could indicate that solar illumination plays a role in controlling the plasma density.

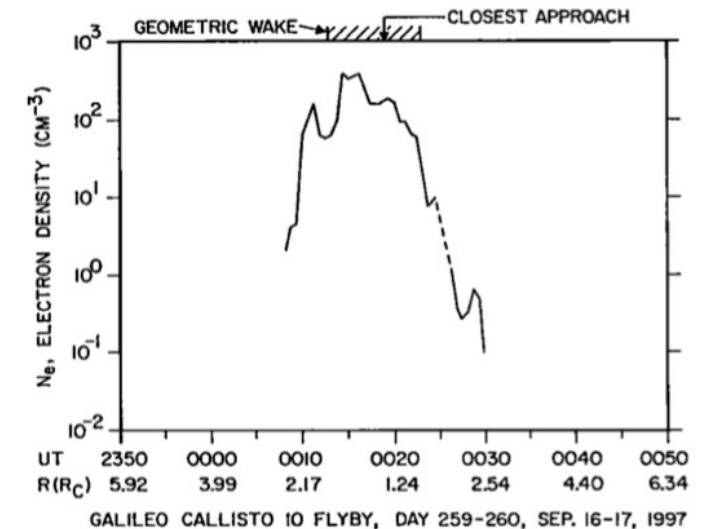


Fig. Electron density profiles determined from the upper hybrid resonance frequency during the C10 flyby. ([Gurnett et al.](#) (2000))

## 1-3-3. Europa ionosphere

Radio occultation [Galileo] ([Kliore et al. \(1997\)](#))

Maximum electron densities ...  $9000 \pm 4000/\text{cc}$

Scale height ...  $240 \pm 40 \text{ km} (\sim 300 \text{ km})$   
 $440 \pm 60 \text{ km} (300 \text{ km} \sim)$

Strong detection ... 5 times

Weak detection ... 1 times

Non\_detection ... 2 times

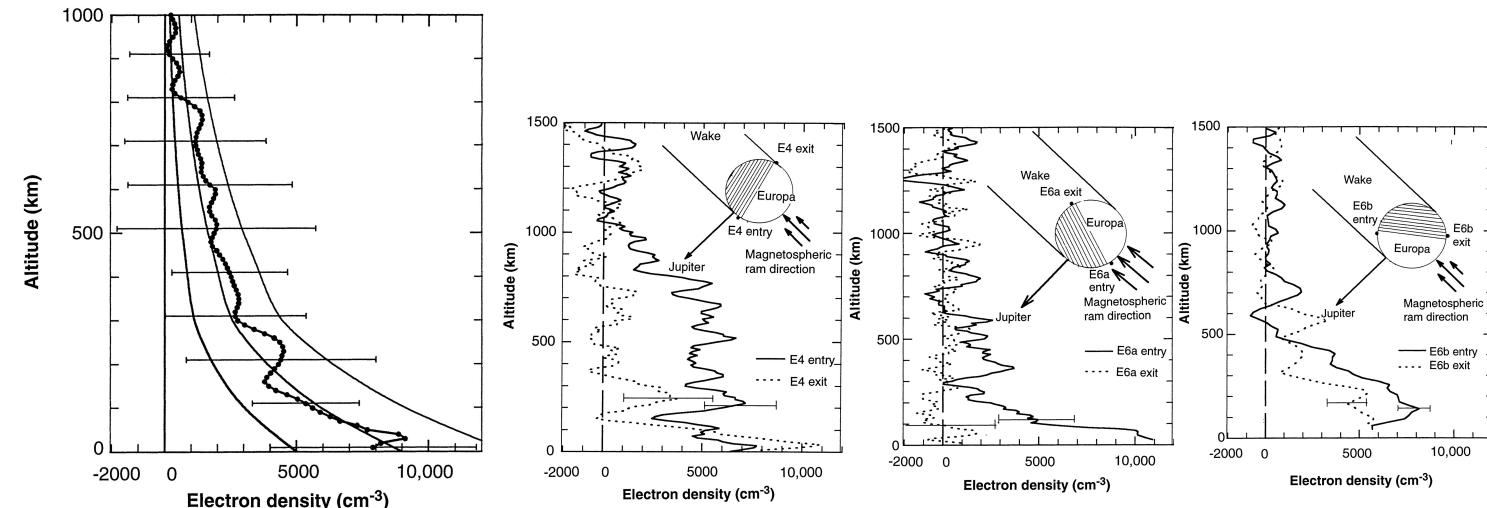


Fig. Average Europa electron density profile computed from the five observations in which an ionosphere was detected.(Kliore et al. 1997)

Fig. Electron density profiles for Europa. (E4, E6a and E6b) (Kliore et al. 1997)

[Kliore et al. \(2001\)](#)

- in order for an ionosphere to be observed, the trailing hemisphere of the satellite **must be in sunlight**
- the atmosphere created by sputtering effects of the Jovian magnetosphere can be **ionized by solar EUV to produce an observable ionosphere.**



- the electron impact ionization rate is  $1.9 \times 10^{-6} \text{ s}^{-1}$  & a solar maximum photoionization rate is  $3 \times 10^{-8} \text{ s}^{-1}$  ([Saur et al. \(1998\)](#))
- It is therefore very difficult to understand why the existence of an ionosphere should depend on solar illumination. ([McGrath et al. \(2009\)](#))

## 1-3-3. Europa ionosphere

In-situ observation of Galileo flyby [Galileo plasma-wave instrument] (Fig.)

The maximum density enhancement observation on any flyby

…  $600 \text{ (cm}^{-3})$  at E12 flyby ([Kurth et al. \(2001\)](#))

The maximum density enhancement observation as the spacecraft entered the wake.

…  $200 \text{ (cm}^{-3}) \Rightarrow 400 \text{ (cm}^{-3})$  at E15 flyby ([McGrath et al. \(2009\)](#))

Flyby	Time of closest approach	Alt. (km)	Upstream/ wake	Magnetic latitude ( $^{\circ}$ )	$\lambda_{\text{III}}$ ( $^{\circ}$ )	LT <sup>a</sup> (h)	Day/night	Jupiter/Anti-ju hemisphere
E4	Dec. 19, 1996 0652:58	692	Wake	6.6	157	16.7	Night	Jupiter
E6	Feb. 20, 1997 1706:10	586	Upstream	-7.6	340	12.9	Night	Jupiter
E11	Nov. 6, 1997 2031:44	2043	Wake	8.7	223	11.0	Day	Anti-Jupiter
E12	Dec. 16, 1997 1203:20	201	Upstream	0.9	118	14.7	Day	Anti-Jupiter
E14	Mar. 29, 1998 1321:05	1644	Upstream	9.1	184	14.4	Day	Anti-Jupiter
E15	May 31, 1998 2112:57	2515	Wake	-0.5	293	10.1	Day	Anti-Jupiter
E17	Sep. 26, 1998 0354:20	3582	Wake	3.6	138	9.9	Day	Anti-Jupiter
E19	Feb. 1, 1999 0219:50	1439	Upstream	5.6	256	9.8	Night	Jupiter
E26	Jan. 3, 2000 1759:43	198	Flux tube	-9.6	2	2.9	Night	Jupiter

<sup>a</sup>Local time with respect to Jupiter.

Fig. Galileo Europa flyby geometric. ([Kurth et al. \(2001\)](#))

The origin and characteristics of Europa ionosphere are still very poorly understood.

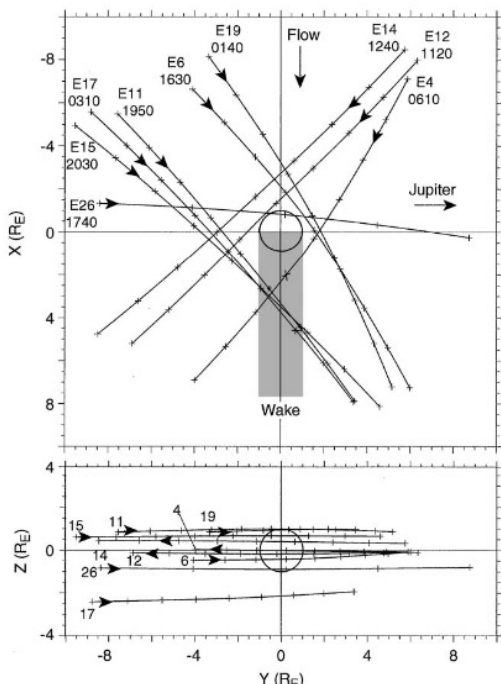


Fig. The geometry of nine Galileo flybys of Europa. ([Kurth et al. \(2001\)](#))

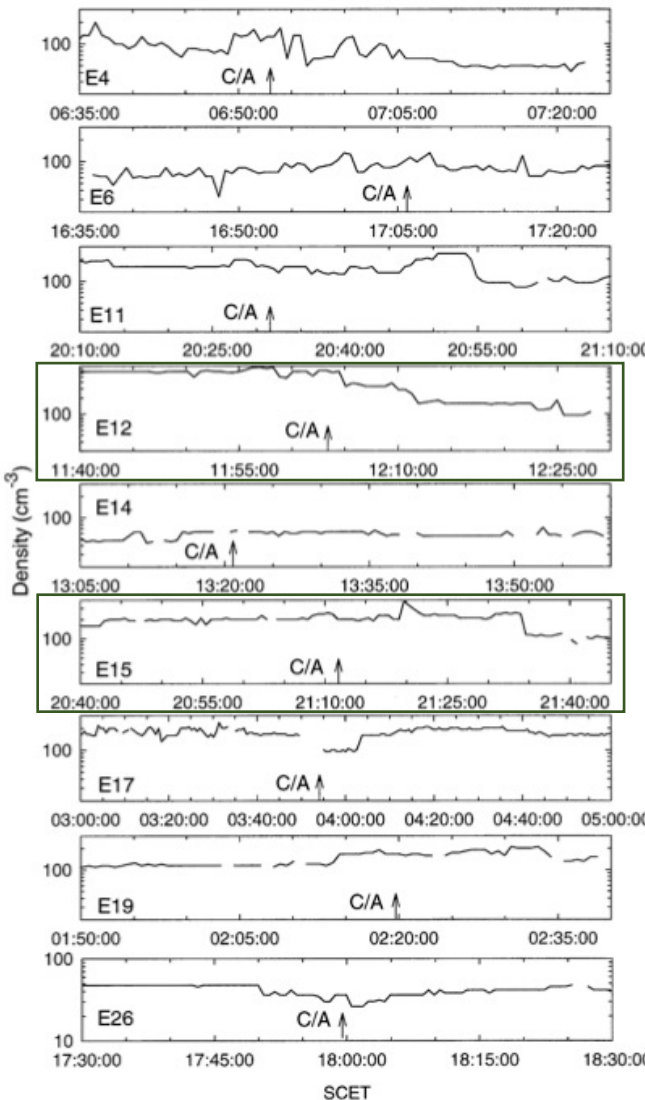
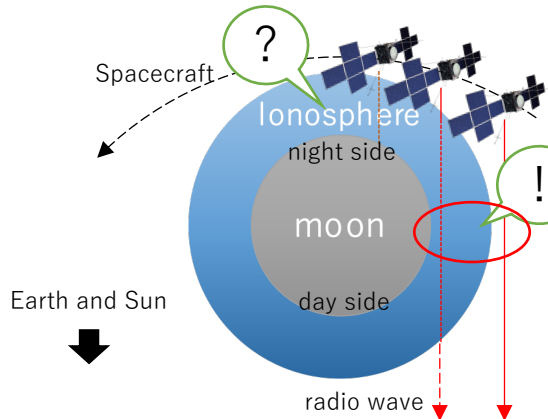


Fig. Electron density profiles based on the upper hybrid resonance band observed during each of Europa flyby. ([Kurth et al. \(2001\)](#))

## 1-3-4. Problems with the previous observation methods

### Radio occultation

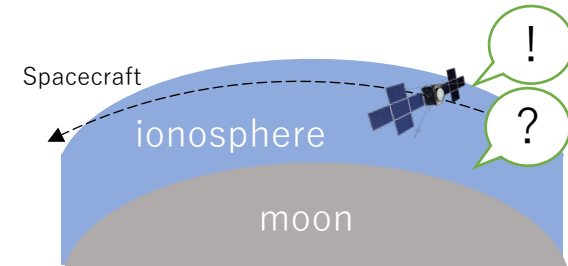


Only ionosphere around day–night boundary

- difficult to evaluate photo-ionization process
- difficult to detect the differences between leading and trailing hemisphere (depend on the positions of the moon, Jupiter and sun)

Fig. Radio observation using spacecraft radio

### In-situ observation

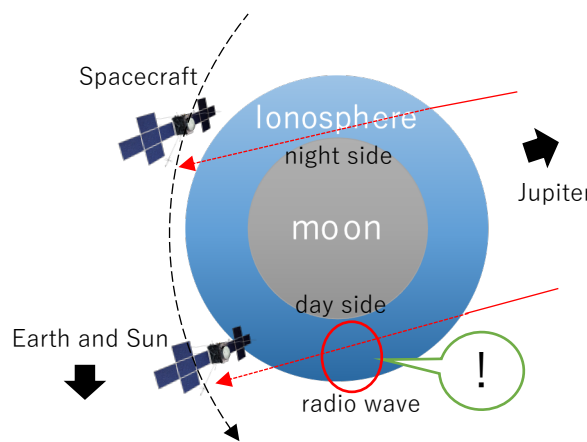


Lack of information at low altitude

- difficult to measure the vertical ionospheric profiles

Fig. In-situ observation

### Jovian radio occultation



Contribute to ...

- estimate the distribution of neutral atmosphere (and plume)
- identify what the origin of icy moons' ionosphere is

Fig. Radio observation using jovian radio

## Occultation modeling using ExPRES Jovian Radio Emission Simulations [Cecconi et al, 2021]

※ Assuming a straight-line propagation (no refraction)

- At lower frequencies, the occultation spectral egress occurs later than predicted. (Fig. 10)
- This prediction mismatch indicates that propagation effects play an important role in the fine understanding of the radio occultation near Galilean moons.

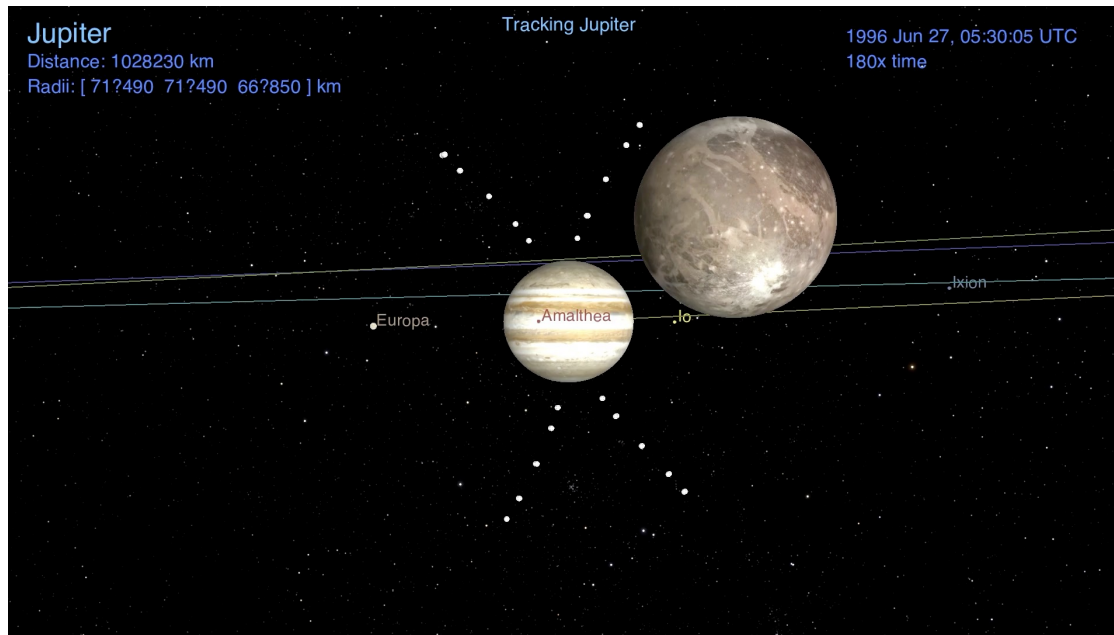


Fig.9 Flyby visualized in the Cosmographia tool. The scene is set with an observer on the Galileo spacecraft, pointing to Jupiter. Ganymede is in the field of view. The ExPRES-modelled visible radio sources are also shown, at 700 kHz, 1 MHz, 2 MHz, 5 MHz and 10 MHz as white dots. The radio sources are conventionally grouped in four sets (named A, B, C and D). [Cecconi et al, 2021]

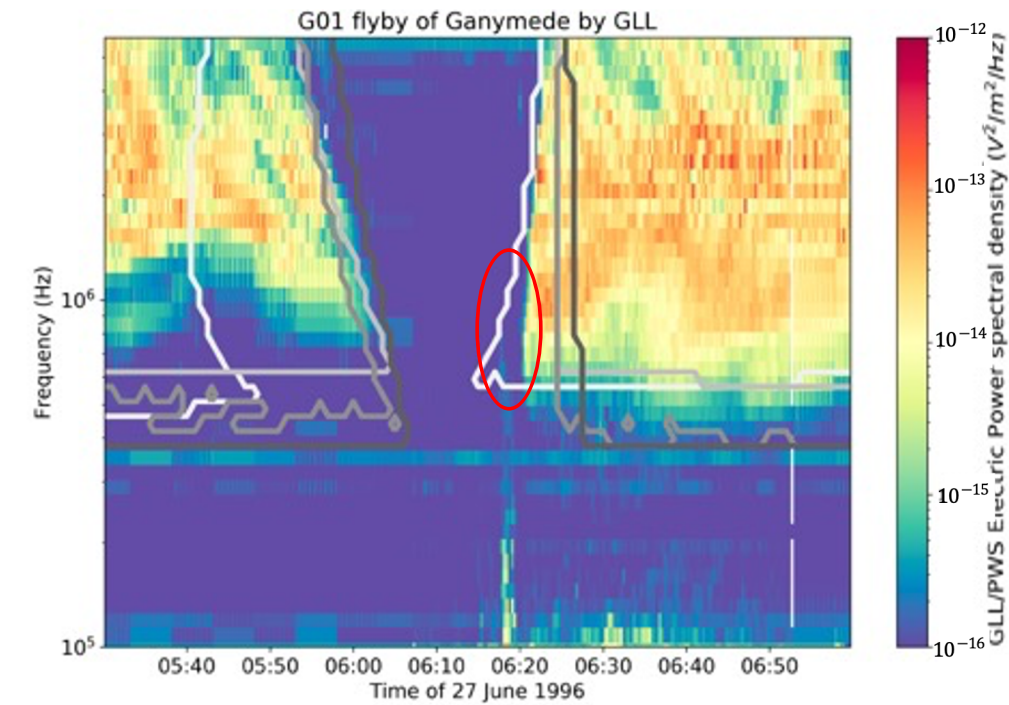


Fig.10 Superimposed Galileo PWS data and ExPRES simulations during Jovian radio emission occultations by Ganymede . The four types of emission (A, B, C, D) are separated (from white to darkgrey, resp.) [Cecconi et al, 2021]

- To investigate spatial structures of ionosphere and plumes created from the water oceanic materials, developing the numerical simulation code for the radar explorations using natural radio waves. [Fig. 4]  
(Collaborative research with institutions in France and Sweden)
- Finally, we will also investigate spatial structures of the interior. [Fig. 5]



## ① Radio occultation observation

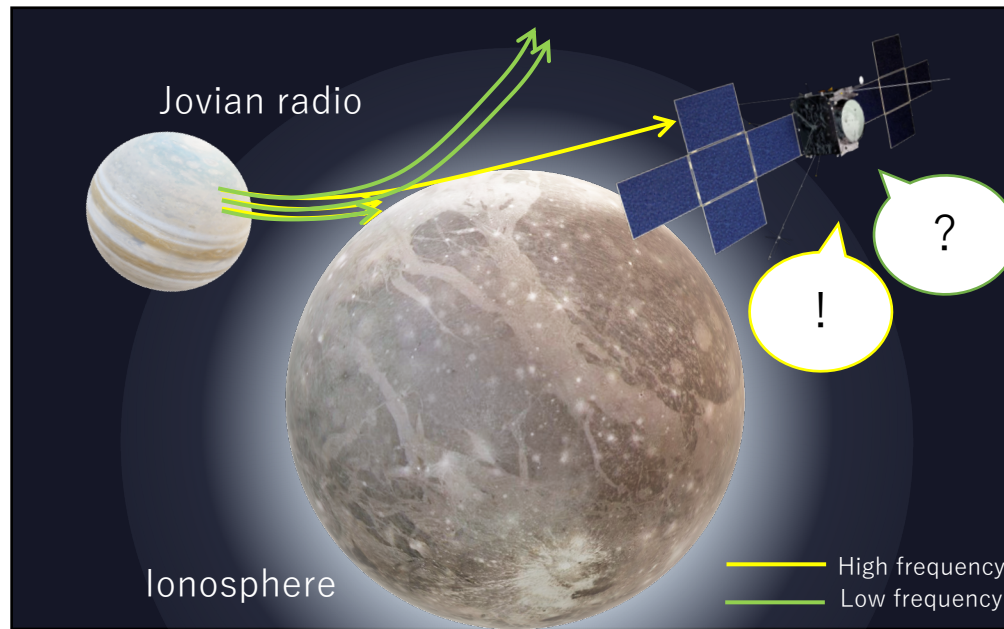


Fig.4 Radio observation using Jovian radio refraction (adapted from Airbus DS and NASA/JPL)

## ② Passive radar

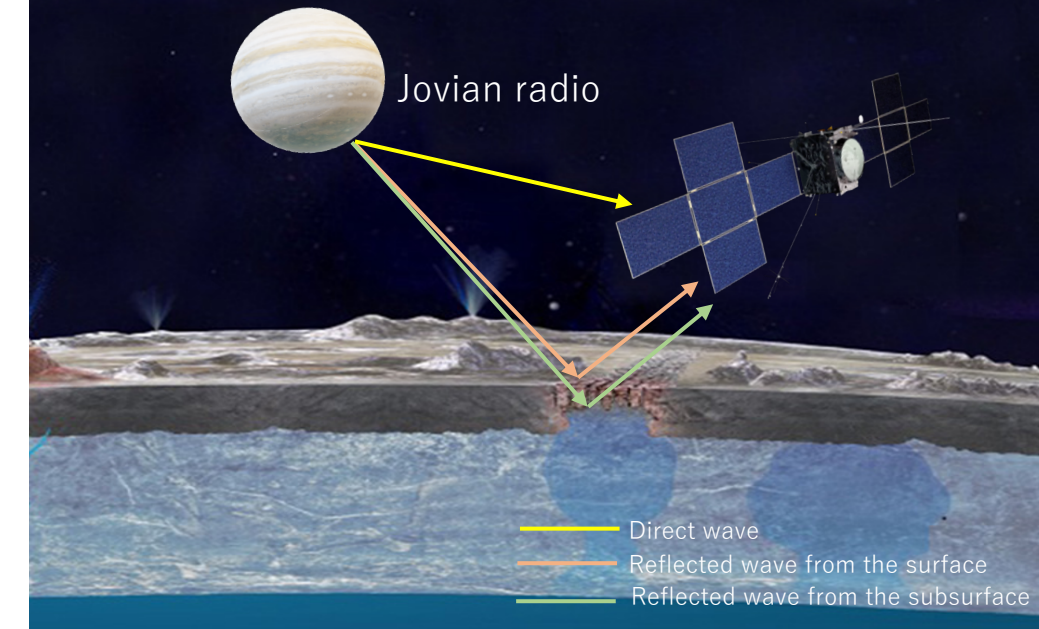


Fig.5 Radio observation using Jovian radio reflection (adapted from NASA/JPL, Airbus DS and gcoe-earths.org)

Today's topic..

- Emulate occultation of the Jovian radio waves during the flybys of the Galileo spacecraft to Ganymede including the ionospheric refraction effect**
- Propose the vertical ionospheric profiles at the altitude below the orbiter**